HIROSAKI UNIVERSITY

Radiation Emergency Medicine 2015 Vol. 4 No. 1 34-39

REM
Radiation Emergency Medicine

Regular Article

A Method for Reducing Skin Dose under IVR Pulsed Fluoroscopic X-ray Irradiation

Kohsei Kudo[1]*, Minoru Osanai[1], Junichi Hirota[1], Sachio Sato[2], Satoshi Naraki[2], Katumasa Suzaki[2], Akira Fujimori[2], Yoshihiro Takai[2, 3] and Yoichiro Hosokawa[1]

[1]*Hirosaki University Graduate School of Health Sciences, 66-1 Hon-cho, Hirosaki, Aomori 036-8564, Japan*
[2]*Department of Radiology, Hirosaki University School of Medicine and Hospital, 53 Hon-cho, Hirosaki, Aomori 036-8563, Japan*
[3]*Department of Radiology and Radiation Oncology, Hirosaki University Graduate School of Medicine, 5 Zaifu-cho, Hirosaki, Aomori 036-8562, Japan*

Received 19 September 2014; revised 13 November 2014; accepted 27 December 2014

Interventional radiology (IVR) procedures are indispensable in treatment directly connected to lifesaving. As IVR requires X-ray irradiation for a long time and is carried out repeatedly, the skin dose to the patient is high. We measured waveforms of the entrance surface dose in pulsed fluoroscopy with the intent of reducing the exposure dose from IVR. Using a flat-panel detector (FPD) system, we also measured entrance surface doses in various cases in normal- and low-dose modes. As a result, wavetail cutoff of waveforms was confirmed. In addition, we confirmed that in each of the cases of lower pulse rates, lower frame rates, larger FPD sizes, larger irradiation fields, shorter table-FPD distances, and thinner phantom thicknesses, doses decreased. Based on these results, from the perspective of reducing exposure doses, fluoroscopy or exposure should be undertaken using: a low pulse rate; a low frame rate during exposure; a large FPD size without magnification; an irradiation field that is not small; and an FPD brought to close to the patient.

Key words: pulsed fluoroscopy, flat-panel detector, interventional radiology, radiation dose

1. Introduction

Interventional radiology (IVR) technologies such as fluoroscopy-guided arterial embolization[1)] and angioplasty through the lower extremity for arterial embolism[2)] were developed by Margulis *et al*.[3)]. The application of IVR procedures in medical treatment has increased markedly, because the procedures offer treatment directly connected to lifesaving, as represented by treatments such as percutaneous coronary intervention (PCI) and percutaneous transluminal coronary angioplasty (PTCA) for myocardial infarction.[4)] IVR, however, requires long periods of X-ray fluoroscopy and repeated exposures because of the handling techniques for the procedures. Furthermore, IVR procedures are repeatedly performed on the same region of the body in many cases. Around 1990, the concern was raised that IVR procedures result in the patient receiving a high exposure dose that can cause radiation-induced skin injuries. The Food and Drug Administration (FDA) issued a warning about reducing exposure doses and preventing radiation-induced skin

*Kohsei Kudo, Ph.D.: Hirosaki University Graduate School of Health Sciences, 66-1 Hon-cho, Hirosaki, Aomori 036-8564, Japan
E-mail: kohsei@cc.hirosaki-u.ac.jp

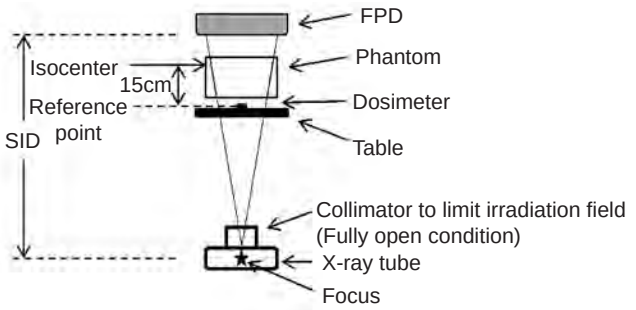

Fig. 1. Geometry for phantom surface dose measurements at the interventional reference point.

injuries in 1994[5]. A case of radiation-induced skin injuries was reported in 1990, involving a 40-year-old man who experienced development of an ulcer on the skin after PTCA, eventually requiring skin grafting. In that case, the estimated absorbed dose exceeded 20 Gy[4, 6]. Fourteen cases of radiation-induced skin injuries caused by IVR performed between 1993-1999 were reported in Japan.[7] The integral skin dose in these cases was estimated to range from only several Gy to 60 Gy. A skin dose close to a threshold dose of 18 Gy within an integrated time of 30 min is thought to be a risk for skin necrosis; this risk varies according to fluoroscopy conditions and the focus-skin distance. However, exposure doses were not measured in almost all cases; therefore, in order to prevent radiation-induced skin injuries, it was necessary to reduce the skin doses. To reduce the exposure dose in IVR procedures, pulsed fluoroscopy can be used. Pulsed fluoroscopic X-rays differ from continuous fluoroscopic X-rays in that the wavetail cutoff is applied to the former at the time of radiation irradiation[8, 9]. In addition, a flat-panel detector (FPD) can be used for an IVR X-ray system, instead of an image intensifier (II)[10-16]. FPDs have good fundamental performance of spatial resolution and detective quantum efficiency compared with IIs.

We measured waveforms of entrance surface doses in pulsed fluoroscopy for the purpose of dose reduction. Using an FPD, we also measured entrance surface doses in cases where the pulse rate in pulsed fluoroscopy, the frame rate in pulsed exposure, FPD size, irradiation field, table-FPD distance, and phantom thicknesses were varied in normal-dose mode (Normal mode) and low-dose mode (Low mode).

2. Materials and Methods

2.1. Method for measuring wavetail waveforms and measurement conditions

A Magic Max dosimeter (IBA, Schwarzenbruck, Germany) (0.01 mGy-15 Gy, 0.1 mGy/s-0.05 Gy/s) was used. All parts of this dosimeter are constructed according to IEC 61674. The type of detector is a semiconductor and this dosimeter can measure tube voltage (kV), practical peak voltage, half-value layer (HVL) of aluminum (Al), dose, dose rate, dose per pulse, exposure time, and waveform.

As general radiographic X-ray equipment, a UD150B-40 system (Shimadzu, Kyoto, Japan) was used. In this case, exposure conditions were an over-table tube, with a source to image receptor distance (SID) of 150 cm taken and without phantom. Waveforms with no wavetail cutoff were measured at tube current (mA) 100 mA and 630 mA.

As continuous fluorographic X-ray equipment, an Ultimax-I DREX-U180 system (Toshiba, Tochigi, Japan) was used. In this case, an under-table tube was used, as shown in Figure 1. Thickness of the Tough Water phantom (Kyoto Kagaku Co., Kyoto, Japan) was 20 cm, with an SID of 86.5 cm, and a table-FPD distance of 30 cm. Measurements were carried out at the interventional reference point (IRP)[17]. Waveforms for no wavetail cutoff were measured under automatic brightness control mode with automatically set kV, mA regulation, and 5 s of fluoroscopy time.

As pulsed fluorographic X-ray equipment, an FPD system (INNOVA IGS630; GE Healthcare, Tokyo, Japan) using cesium iodide as the detector was used. This equipment was loaded with. In this case, an under-table tube was used (Fig. 1). The arrangement and measurement points were the same as those in the case of continuous fluoroscopic X-rays. Waveforms of wavetail cutoff by triode X-ray tube were measured with automatic kV-mA regulation, 7.5 pulses/s (pps) in Normal mode for high image quality or Low mode for low dose.

2.2. Measurement of entrance dose on the phantom surface

Magic Max was used as a dosimeter, and INNOVAIGS630 was used as the device.

Dose rates were measured while changing the pulsed fluoroscopic rate (7.5, 15, or 30 pps) or frame rate [15 or 30 frames/s (fps)]. In each case, the dose rates in Normal mode and Low mode were measured. Arrangement and measurement points were the same as in the pulsed fluoroscopic X-rays described in 2.1 above. Exposure dose rates were automatically regulated.

Next, dose rates were measured at a fluoroscopic pulse rate of 15pps, changing the FPD size (30×30, 20×20, 16×16, or 12×12 cm^2), irradiation field [maximum, half-maximum (1/2), quarter-maximum (1/4)], table-FPD distance (30, 40, or 50 cm), and phantom thickness (20, 22, or 25 cm) in various combinations. In each case, dose rates in Normal and Low mode were measured. Arrangement and measurement points were the same as those for pulsed fluoroscopic X-rays as described in 2.1

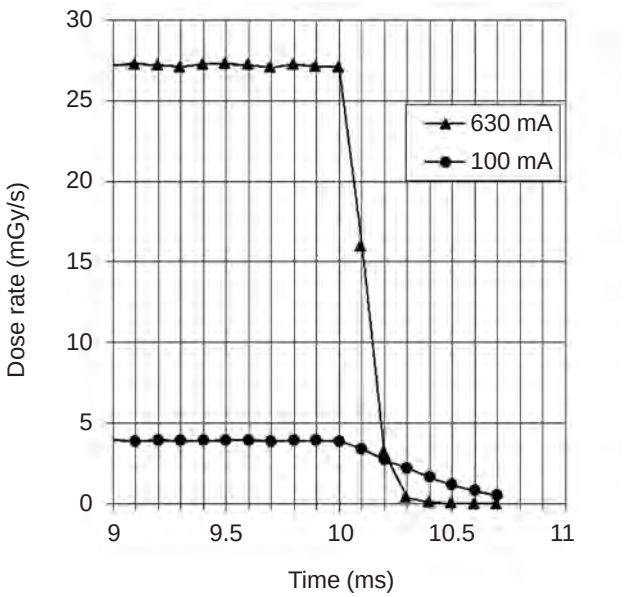

Fig. 2. Waveforms of no wavetail cutoff general radiographic X-rays. Dose rates at both 630 mA and 100 mA of tube current started to fall 10 ms after irradiation. Falling time was longer at 100 mA than at 630 mA. Tube-voltage, 80 kV.

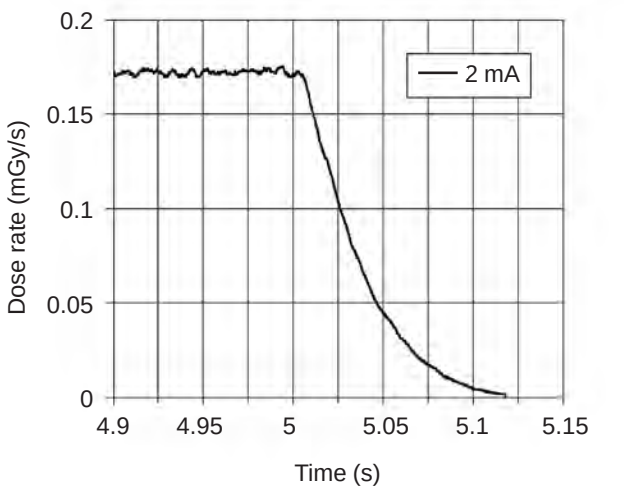

Fig. 3. Waveforms of no wavetail cutoff continuous fluoroscopic X-rays. Wavetails after 5 s were long, and falling time was approximately 100 ms. Tube-voltage: 88 kV.

above. Exposure dose rates were automatically regulated.

Pulsed fluoroscopy time was about 10 s in all cases. Data are expressed as the mean ± standard deviation (SD) obtained from three measurements.

3. Results

3.1. Measurement of wavetail waveforms

Waveforms of no wavetail cutoff for general radiographic X-rays are shown in Figure 2. Dose rates during irradiation were 27 mGy/s at a tube current of 630 mA and 3.9 mGy/s at 100 mA. Dose rates at both 630 mA and 100 mA of tube current started to fall 10 ms after irradiation. This study defined falling time as the time until 5% of the peak dose rate was reached. Falling time was 0.3 ms at 630 mA, and 0.7 ms at 100 mA.

Waveforms for no wavetail cutoff continuous fluoroscopic X-rays are shown in Figure 3. Dose rates until 5 s had passed were about 0.17 mGy/s. Wavetails after 5 s were long, and falling time was approximately 100 ms.

Waveforms of wavetail cutoff pulsed fluoroscopic X-rays are shown in Figure 4. Dose rates of pulses in Normal mode and Low mode were 1.90 mGy/s and 0.74 mGy/s, respectively. Falling time for wavetails in both modes was short, at 0.3 ms.

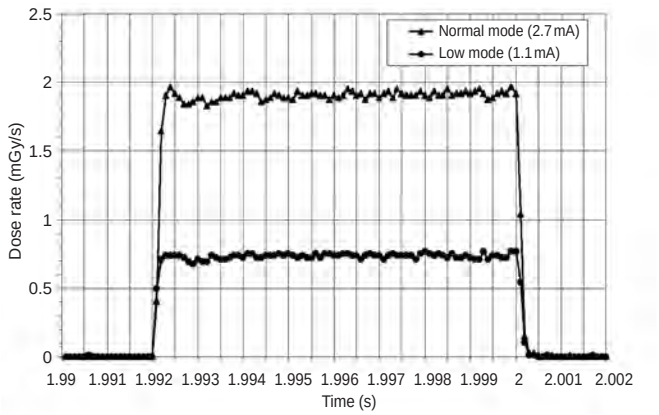

Fig. 4. Waveforms of wavetail cutoff pulsed fluoroscopic X-rays. Dose rate falling times for wavetails in both modes were short, and falling time was 0.3 ms. Tube-voltages at Normal mode and Low mode were 80 and 81 kV, respectively.

3.2. Measurement of entrance dose on the phantom surface

The relationship between pulse rate and dose rate is shown in Figure 5A. In cases where pulse rates were lowered, doses fell in both Normal mode and Low mode. Dose rates at 30, 15 and 7.5 pps in Normal mode were 0.232 ± 0.0009, 0.172 ± 0.0002, and 0.114 ± 0.0001 mGy/s, respectively. Dose rates at 30, 15 and 7.5 pps in Low mode were 0.0894 ± 0.00041, 0.0677 ± 0.00008, and 0.0452 ± 0.00009 mGy/s, respectively. On the other hand, ratios of dose rates in Normal mode and Low mode were constant.

The relationship between exposure frame rate and dose rate is shown in Figure 5B. In both Normal and Low mode, dose rates in the case of a lower frame rate were lower. Dose rates in Normal mode (30, 15 fps) were 1.22 ± 0.001 and 0.633 ± 0.0011 mGy/s, respectively. Dose rates in Low mode (30, 15fps) were 0.669 ± 0.0023 and 0.347 ± 0.0003 mGy/s. Ratios of dose rates in Normal mode and Low mode were constant.

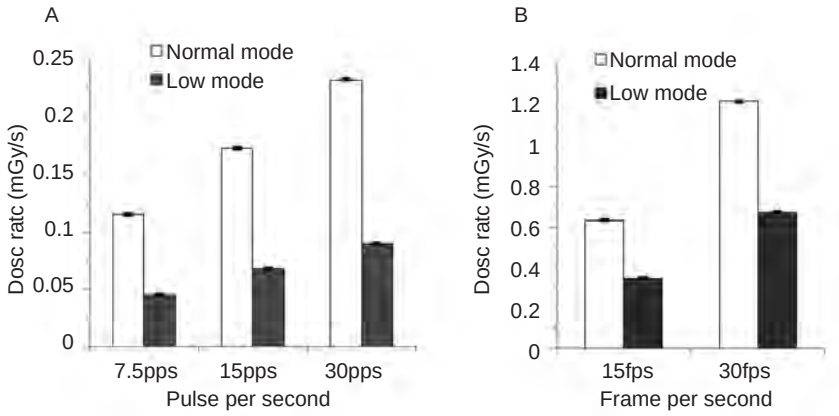

Fig. 5. A) Relationship between pulse rate and dose rate. **B)** Relationship between exposure frame rate and dose rate. Data are expressed as mean±SD of three measurements.

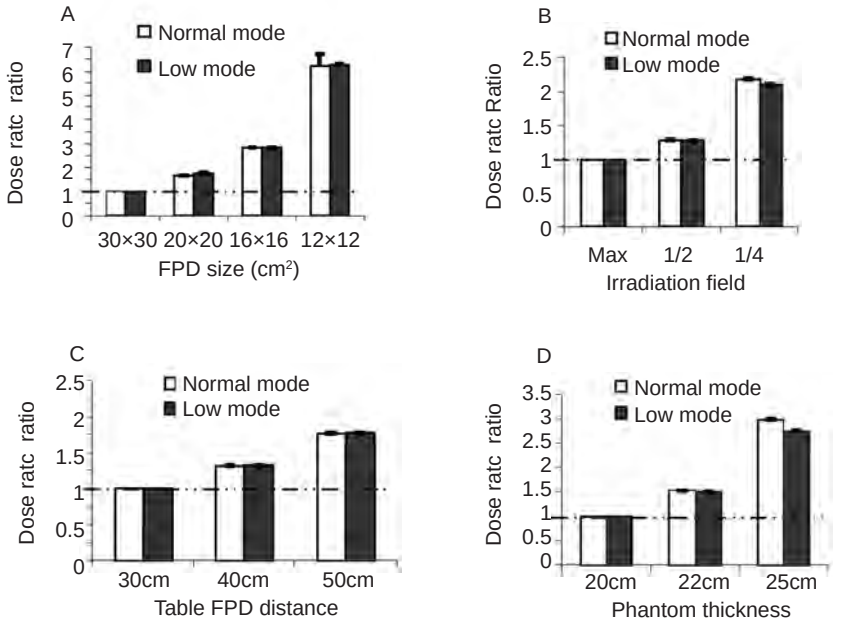

Fig. 6. A) Relationship between FPD size and dose rate ratio. **B)** Relationship between irradiation field and dose rate ratio. **C)** Relationship between table-FPD distance and dose rate ratio. **D)** Relation between phantom thickness and dose rate ratio. Data are expressed as mean ± SD of three measurements.

The relationship between FPD size and dose rate ratio is shown in Figure 6A. In both Normal and Low mode, when FPD size was decreased, dose ratio increased. Dose rate ratios for an FPD size of 20×20 were 1.7 in Normal mode and 1.8 in Low mode. Dose rate ratio for the FPD size of 16×16 was 2.8 in both Normal and Low mode. Dose rate ratios for the FPD size of 12×12 were 6.2 in Normal mode and 6.3 in Low mode, representing quite high values.

The relationship between irradiation field and dose rate ratio is shown in Figure 6B. When an irradiation field was decreased, the dose rate ratio increased. The dose rate ratio in a 1/2 field was 1.3 in both Normal mode and Low mode. Dose rate ratio in a 1/4 field was 2.2 in Normal mode and 2.1 in Low mode.

The relationship between table-FPD distances and dose rate ratio is shown in Figure 6C. When table-FPD distance was increased, dose rate ratio increased in both Normal mode and Low mode. Dose rate ratio was 1.3 in both Normal and Low modes at a table-FPD distance of 40 cm, and 1.8 at a table-FPD distance of 50 cm in both modes.

The relationship between phantom thicknesses and dose rate ratio is shown in Figure 6D. When phantom thickness was increased, dose rate ratio increased in both Normal and Low modes. Dose rate ratio with a phantom

thickness of 22 cm was 1.5 in both Normal and Low mode. Dose rate ratios with a phantom thickness of 25 cm were 3.0 in Normal mode and 2.7 in Low mode.

4. Discussion

We confirmed wavetail cutoff in pulsed fluoroscopy on the basis of waveforms. With no wavetail cutoff (Figs. 2, 3), falling time depended on tube current. This is due to the effect of diode vacuum tube characteristics.[8] On the other hand, for waveforms in pulsed fluoroscopy with wavetail cut off by triode tube, although tube current was low, falling time was 0.3 ms (Fig. 4). Furthermore, falling time did not depend on tube current. Dose of wavetail is unnecessary irradiation for diagnostic imaging. We confirmed that wavetail cutoff reduces invalid exposure.

At low pulse rates, measurements were carried out to clarify whether doses were reduced (Fig. 5A). When pulse rates were lowered, dose rate ratios dropped. However, ratios of pulses per second were not proportional to ratios of dose rates. For example, the ratio of 30 pps and 7.5 pps was 4:1, but the ratio of dose rates was 2:1. When pulse rates were decreased to low values, pulse width or tube current increased in some cases. Dose rates may not therefore be proportional to pulse rate as mentioned above, depending on the device[18, 19]. Regarding radiographic frame rates (Fig. 5B), ratios of frame rates were proportional to ratios of dose rates, representing the same result described in the Guidelines for Radiation Safety in Interventional Cardiology[19].

When FPD sizes were decreased, dose rate ratios increased (Fig. 6A). The FPDs used were an indirect conversion type. When FPD size was decreased to magnify an image, noise became conspicuous, requiring an increased dose[20]. A specific amount of dose per unit area is thus considered to be needed for image magnification. For example, the area ratio of the FPD size of 12×12 was $(30 \times 30)/(12 \times 12) = 6.3$, and the dose rate ratio was 6.2 in Normal mode. The area ratio became close to the dose rate ratio. We consider that image magnification should only be used when necessary.

When irradiation fields were decreased, dose rate ratios increased (Fig. 6B). Regarding this matter, dose ratio is not reported to change[19], because the image is not magnified and the display range on the monitor is merely narrowed. Our results differed from the findings of that report. In this case, we thought that the quantity of scattered rays from a phantom was decreased by making the irradiation field smaller. That is, since the incident dose to the FPD decreases, dose is increased to compensate for the decrement. In our data, the dose rate ratio in a 1/4 irradiation field was about doubled. The irradiation field therefore should not be decreased unless it is necessary for diagnosis.

When table-FPD distances were increased, dose rate ratios increased (Fig. 6C). In cases where table-FPD distance was increased, so too was SID. Incident dose into the FPD therefore decreased. The abovementioned increase is considered to be a result of compensation for the decrease. According to the inverse-square law for distance, in the case of a table-FPD distance of 30–40 cm (SID, 86.5–96.5 cm), $(96.5/86.5)^2 = 1.2$ was found, and the dose rate ratio was 1.3. In the case of a table-FPD distance of 30–50 cm (SID, 86.5–106.5 cm), $(106.5/86.5)^2 = 1.5$ was found, and the dose ratio was 1.8. Dose rate ratios were higher than values calculated according to the inverse-square law of distance. Scattered rays from a phantom also decrease with distance from the FPD in those cases. To compensate for the decrease, X-rays is considered to be increased.

When phantom thickness was increased, the dose rate ratio became higher (Fig. 6D). Attenuation of X-rays increases with increased phantom thickness. Accordingly, the incident dose to the FPD is also decreased, as a matter of course. For confirmation, we calculated attenuation ratios for each phantom thickness. Attenuation ratios were calculated from the attenuation coefficient of water data from the National Institute of Standards and Technology[21] at an effective energy[22] with HVL (Al). Attenuation ratios calculated at 20, 22 and 25 cm in Normal mode were 1.0, 1.6 and 3.3, respectively, and measured dose rate ratios were 1.0, 1.5 and 3.0. On the other hand, in Low mode the calculated attenuation ratios were 1.0, 1.6 and 3.2, and measured dose rate ratios were 1.0, 1.5 and 2.7. Calculated values were higher at 25 cm. This is considered to be because scattered rays from the phantom increased, unlike the case with table-FPD distance.

As the points of focus, in each of the cases of lower pulse rates, lower frame rates, larger FPD sizes, larger irradiation fields, shorter table-FPD distances, and thinner phantom thicknesses, doses decreased. In particular, in our data, the dose rate ratio in a 1/4 irradiation field was about doubled, and a dose rate in the case of a 12×12 cm^2 FPD exceeds six times the dose rate with a 30×30 FPD.

From the abovementioned results, we consider that, from the perspective of reducing exposure dose, when IVR is carried out, fluoroscopy or exposure should be performed using the following conditions: Low mode; low pulse rate; low frame rate during exposure; large FPD size without magnification; no decrease in irradiation field; and FPD close to the patient.

5. Conclusion

We measured waveforms in pulsed fluoroscopy, and confirmed wavetail cutoff therein. Furthermore, we confirmed that each or a combination of lower pulse

rate, lower frame rate, larger FPD, larger irradiation field, shorter table-FPD distance, and thinner phantom thickness resulted in decreased dose. As presented in this study, the exposure dose to the patient can be reduced by understanding the characteristics of the device being used. Image quality depends on the X-ray dose, but X-ray dose can still be minimized without affecting diagnosis in actual procedures for IVR.

Acknowledgments

We would like to thank everyone in the Department of Radiology at Hirosaki University School of Medicine and Hospital for cooperating with for our study.

References

1. Luessenhop AJ and Spence WT (1960) Artificial embolization of cerebral arteries. Report of use in a case of arteriovenous malformation. J Am Med Assoc 172:1153–1155.
2. Dotter CT and Judkins MP (1964) Transluminal treatment of arteriosclerotic obstruction. Description of a new technic and a preliminary report of its application. Circulation 30:654–670.
3. Margulis AR (1967) Interventional diagnostic radiology. A new subspeciality. Am J Roentogenol 99:761–762.
4. ICRP (2000) Publication 85. Avoidance of radiation injuries from medical interventional procedures. The International Commission on Radiological Protection, Sweden.
5. FDA (1994) Avoidance of Serious X-Ray-Induced Skin Injuries to Patients During Fluoroscopically-Guided Procedures. Food and Drug Administration, USA.
6. Shope TB. Radiation-induced Skin Injuries from Fluoroscopy. FDA. Available from: http://www.fda.gov/radiation-emittingproducts/radiationemittingproductsandprocedures/medicalimaging/medicalx-rays/ucm116682.htm.
7. Togashi A (2001) Considering of Radiation Protection from the Report on the Dermatopathy by IVR. Nihon Houshasen Gijutsu Gakkai Zasshi 57:1444–1450. (in Japanese)
8. Takano H, et al. (2001) High-speed pulse fluoroscopic system with high-voltage semiconductor switching modules. Nihon Houshasen Gijutsu Gakkai Zasshi 57:1209–1217. (in Japanese)
9. Chida K, et al. (2001) Comparison of pulsed fluoroscopy by direct control using a grid-controlled X-ray tube with pulsed fluoroscopy by primary control. Nihon Houshasen Gijutsu Gakkai Zasshi 57:1534–1540. (in Japanese)
10. Holmes DR Jr, et al. (2004) Flat-panel detectors in the cardiac catheterization laboratory: revolution or evolution—what are the issues? Catheter Cardiovasc Interv 63:324 –330.
11. Tsapaki V, et al. (2004) Dose performance evaluation of a charge coupled device and a flat-panel digital fluoroscopy system recently installed in an interventional cardiology laboratory. Radiat Prot Dosimetry 111:297–304.
12. Tsapaki V, et al. (2004) Comparison of a conventional and a flat-panel digital system in interventional cardiology procedures. Br J Radiol 77:562–567.
13. Suzuki S, et al. (2005) Radiation dose to patients and radiologists during transcatheter arterial embolization: comparison of a digital flat-panel system and conventional unit. Am J Roentgenol 185:855–859.
14. Davies AG, et al. (2007) Do flat detector cardiac x-ray systems convey advantages over image-intensifier-based systems? Study comparing x-ray dose and image quality. Eur Radiol 17:1787–1794.
15. Kato K, et al. (2010) Patient radiation dose in percutaneous coronary intervention. Shinzo 42:1285–1293. (in Japanese)
16. Chida K, et al. (2009) Radiation dose of interventional radiology system using a flat-panel detector. Am J Roentgenol 193:1680–1685.
17. IEC 60601-2-43 (2010) Medical electrical equipment. Particular requirements for basic safety and essential performance of X-ray equipment for interventional procedures. The International Electrotechnical Commission.
18. Japan association on radiological protection in medicine (2004) The Guidelines on prevention of radiation-related skin disorders following interventional radiological procedure − Q&A and Discussion. Booklet series 3, Tokyo. (in Japanese)
19. JCS Joint Working Group (2011) Guideline for Radiation Safety in Interventional Cardiology. Circ J 77:519–549.
20. Kato K, et al. (2011) Reduction Method of Patients' Radiation Dose Considering the Size of Field of View with a Digital Cine X-ray System Loading a Flat-panel Detector. Jpn J Radiological Technology 67:1443–1447. (in Japanese)
21. NIST http://physics.nist.gov/PhysRefData/XrayMassCoef/ComTab/water.html. Accessed August 1, 2014.
22. Shimizu S, et al. (1999) Characteristics of X ray calibration fields for performance test of radiation measuring instruments. JAERI-Tech 99–004:89. (In Japanese)